FRONT SOLUTIONS OF RICHARDS' EQUATION

J.-G. Caputo*), [1,2], Y. A. Stepanyants[3]

1) Laboratoire de Mathématiques, INSA de Rouen, B.P. 8, 76131 Mont-Saint-Aignan cedex, France.

E-mail: caputo@insa-rouen.fr

2) Laboratoire de Physique théorique et modelisation, Université de Cergy-Pontoise and C.N.R.S.

3) Australian Nuclear Science and Technology Organisation, PMB 1, Menai (Sydney), NSW, 2234, Australia, E-mail: Yury.Stepanyants@ansto.gov.au

PACS: 52.35.Tc Shock waves and discontinuities , 47.56.+r Flows through porous media 52.35.Mw Nonlinear phenomena: waves

Keywords: convection-diffusion equation, Burgers equation, front solutions, soil physics, inflitration, imbibition.

Abstract

Front solutions of the one-dimensional Richards' equation used to describe groundwater flow are studied systematically for the three soil retention models known as Brooks–Corey, Mualem–Van Genuchten and Storm–Fujita. Both the infiltration problem when water percolates from the surface into the ground under the influence of gravity and the imbibition (absorption) problem when groundwater diffuses in the horizontal direction without the gravity effect are considered. In general, self-similar solutions of the first kind in the form of the front exist only for the imbibition case; such solutions are stable against small perturbations. In the particular case of the Brooks–Corey model, self-similar solutions of the

second kind in the form of decaying pulse also exist both for the imbibition and infiltration cases. Steady-state solutions in the form of traveling fronts exist for the infiltration case only. The existence of such solutions does not depend on the specifics of the soil retention model. It is shown numerically that these solutions are stable against small perturbations.

Key words: Porous media; groundwater flow; Richards' equation; self-similar solution; steady-state solution; water front stability.

---

*) Corresponding author.

1 Introduction

The basic equation in the theory of groundwater flow through unsaturated porous media is Richards' equation which was suggested in 1931 [7]. This nonlinear convection-diffusion equation can be written as a conservation law for the water content, the quantity of water contained in a given soil volume. The convection term is due to gravity while the diffusive term comes from Darcy's law (see, e.g., [10]. One of the remarkable features of such partial differential equations is the existence of traveling-waves and self-similar solutions (see, e.g., the articles "Diffusion" and "Zeldovich–Frank-Kamenetsky Equation" in the encyclopedia [9]). Another well-known example of nonlinear convection-diffusion equation is the classical Burgers equation (see, e.g., [14]). It can be linearized through the Cole–Hopf transformation and possesses exact analytical solutions.

Travelling wave solutions are also known for the Richards' equation. Their structure depends on the model chosen to represent the soil water retention function. Each model yields a different nonlinearity. In this paper we present a comparative analysis of front wave solutions of Richards' equation for typical soil retention functions. By front solution we mean waves connecting two regions where the water content is different. We consider the infiltration problem where both the convective and diffusive terms are present and the imbibition (or absorption [6]) problem where the convective term is absent, i.e. when water diffuses in the horizontal direction without the effect of gravity.

The three well-known soil retention models known as Brooks–Corey, Mualem–Van Genuchten and Storm–Fujita are used in our study. The first and third models are applicable far and close to the water saturation respectively, whereas the second one covers the whole range of water content. Despite having these different ranges of applicability, these models exhibit qualitatively similar features. Using a travelling wave ansatz we found front solutions for the infiltration problem and in some special cases for the imbibition problem. Self-similar front solutions were found only for the imbibition problem. A numerical study shows that travelling fronts are stable for the infiltration problem whereas self-similar fronts are stable for the imbibition problem.

After introducing the Richards equation and presenting the different models of water retention functions in section 2, we calculate self-similar solutions of the first and second kinds in section 3 and the travelling front solutions in section 4. The stability of the front solutions is investigated numerically in section 5 and we conclude in section 6.

2 Richards' equation and different models of water retention functions

Richards' equation commonly used in the infiltration theory of unsaturated porous media is a simple consequence of two basic equations. The first one is the fundamental mass conservation law

$$\frac{\partial \theta}{\partial t} + \mathrm{div}\mathbf{V}_D = 0, \tag{1}$$

where θ is the volumetric liquid content in the unit volume of a soil (the liquid can be water, oil or something else), and $\mathbf{V}_D$ is the Darcy flux or liquid flow per unit area.

The second equation is a generalization of the empirical Darcy's equation relating the liquid flux, $\mathbf{V}_D$ to the total energy potential $H = \psi - z$ (see for example the book [10])

$$\mathbf{V}_D = -K(\theta)\nabla H = -K(\theta)\nabla\psi + K(\theta)\nabla z, \tag{2}$$

where ∇z is the unit vector directed downward, in the positive direction of

the axis z. The hydraulic conductivity $K(\theta)$ of an unsaturated porous medium can be presented as a the product $K(\theta) = K_s k_r(\theta)$, where $K_s = \kappa g/\nu$ is the saturated hydraulic conductivity in which κ is the medium permeability, g is the acceleration due to gravity and ν is the liquid kinematic viscosity. Another variable, $k_r(\theta)$, is the relative hydraulic conductivity of the unsaturated medium, it depends on the volumetric liquid content and satisfies $0 \leq k_r(\theta) \leq 1$. Note that the Darcy law was established originally for water percolation through saturated soils. Later it was generalized to liquid flow through unsaturated porous media with nonconstant hydraulic conductivity $K(\theta)$ depending on the volumetric liquid content.

By substituting $\mathbf{V}_D$ from Eq. (2) into Eq. (1) one obtains

$$\frac{\partial \theta}{\partial t} = \operatorname{div}\left[K(\theta)\nabla\psi - K(\theta)\nabla z\right]. \tag{3}$$

This is commonly known as Richards' equation [7], while Buckingham [2] derived it almost quarter of century earlier. In essence Eq. (3) is a Fokker–Plank equation as was pointed out firstly by Philip [6].

In the present form the equation is not closed because one must specify the function $K(\theta)$ and indicate the relationship between ψ and θ. To do that, replace first the function θ by the normalized function Θ, called the degree of liquid saturation and defined by (see, e.g., [10])

$$\Theta \equiv \frac{\theta - \theta_r}{\theta_s - \theta_r}, \quad 0 \leq \Theta \leq 1, \tag{4}$$

where θ_r is the residual liquid content in the porous medium which exists practically always on walls of solid skeleton of a porous medium due to molecular forces. A typical value of θ_r for water in a soil is about 0.01 [10]. Another parameter θ_s is the saturated liquid content in a porous medium which corresponds, roughly speaking, to the total volume of a void space in a unit volume of a porous medium. In practice, however, all this volume is unachievable for liquid because usually there is some amount of closed pores where liquid cannot penetrate. The value θ_s depends on the porosity and typically ranges from 0.3 to 0.5 for different soils.

Now we consider the functions $\psi(\Theta)$ and $K(\Theta)$ which are known as soil water retention curves. Two of these are widely used:

1. The Brooks and Corey relation

$$\Theta(\psi) = \left(\frac{\psi}{\psi_b}\right)^{-\lambda}, \quad \text{or} \quad \psi = \psi_b \Theta^{-1/\lambda}, \tag{5}$$

where the parameters ψ_b (the bubbling pressure) and λ (the pore size distribution parameter) are two constants. Their typical range is $-0.26 < \psi_b < -0.073$ and $\lambda > 0$ [10].

For the relative conductivity the following formula is usually used

$$k_r(\psi) = \left(\frac{\psi}{\psi_b}\right)^{-(2+3\lambda)}, \quad \text{or} \quad k_r(\Theta) = \Theta^{\frac{2+3\lambda}{\lambda}}. \tag{6}$$

2. The Van Genuchten (vG) retention relation

$$\Theta(\psi) = \left[1 + \left(\frac{\psi}{\psi_b}\right)^{c}\right]^{-\lambda/c}, \quad \text{or} \quad \psi = \psi_b \left(\Theta^{-c/\lambda} - 1\right)^{1/c}, \tag{7}$$

where c is another fitting parameter. We use this form of vG relationship which is called also a transitional Brooks and Corey (tBC) relationship [10] but in essence it is equivalent to the original Van Genuchten formula [13]. Note that the BC relationship can be treated as an extreme case of the vG one when $c \to \infty$.

For the relationship between k_r and Θ the Mualem's formula [4] will be used in the form

$$k_r(\Theta) = \sqrt{\Theta}\left[1 - \left(1 - \Theta^{c/\lambda}\right)^{\lambda/c}\right]^2. \tag{8}$$

The combination of the two last relationships we call the Mualem–Van Genuchten model.

The dependencies $\psi(\Theta)$ and $k_r(\Theta)$ for both considered models are shown in Figs. 1 and 2. As these dependencies are assumed known, one can rewrite Richards' equation (3) in a closed form in terms of Θ (other forms of Richards equation, e.g., in terms of ψ are also known and widely used [10]):

$$\frac{\partial \theta}{\partial t} = \operatorname{div}\left[D(\theta)\nabla\theta - K(\theta)\nabla z\right], \tag{9}$$

where $D(\theta) = K(\theta)\frac{d\psi}{d\theta}$ is the soil liquid diffusivity [10] and can be treated as a nonlinear diffusion coefficient. Since the functions $K(\Theta)$ and $\psi(\Theta)$ are given, the diffusivity analytical function can be readily calculated,

$$D(\Theta) = K(\Theta)\frac{d\psi}{d\Theta}\frac{d\Theta}{d\theta} = \frac{K(\Theta)}{\theta_s - \theta_r}\frac{d\psi}{d\Theta}.$$

The corresponding expressions for two above mentioned and one more additional model are as follows.

1. BC model:

$$D(\Theta) = D_0\Theta^{2+1/\lambda}, \quad \text{where} \quad D_0 = -\frac{K_s\psi_b}{\lambda(\theta_s - \theta_r)}. \tag{10}$$

   Note that it is assumed in soil physics that ψ and ψ_b are both negative, so that D_0 and $D(\Theta)$ are positive.

2. MvG model:

$$D(\Theta) = D_0\frac{\left[1 - \left(1 - \Theta^{c/\lambda}\right)^{\lambda/c}\right]^2\left(1 - \Theta^{c/\lambda}\right)^{1/c-1}}{\Theta^{1/\lambda+1/2}} \tag{11}$$

3. Another model which is also popular in the soil physics is called Storm–Fujita model [10]. Its popularity is mainly conditioned by the exact analytical solvability of Richards' equation [8], although it can really approximate some kinds of soils for large degree of liquid saturation (see below). The diffusivity function for this model is

$$D(\Theta) = D_0\frac{a}{(b - \Theta)^2}, \tag{12}$$

   where a and $b = 1 + \varepsilon$ with $\varepsilon \ll 1$ are the empirical fitting parameters. The entire Richards' equation for this model will be presented below, and the corresponding dependency for $k_r(\Theta)$ can be reconstructed on the basis of the given equation form:

$$k_r(\Theta) = 1 - \frac{\Lambda}{E} + \frac{\Lambda}{1 + E - \Theta} - \left(1 - \frac{\Lambda}{E}\frac{1}{1+E}\right)(1 - \Theta), \tag{13}$$

   where Λ is the another fitting parameter and $E = \frac{\varepsilon}{\theta_s - \theta_r}$. One can also reconstruct the retention curve $\psi(\Theta)$ on the basis of given functions $k_r(\Theta)$ and $D(\Theta)$. We do not present this dependency here because it is fairly complex and not interesting in the discussed context.

The dependencies $D(\Theta)$ for the three models discussed above are shown in Fig. 3. As one can see from this figure, the diffusivity given by the MvG model

with $\lambda = 1$ and $c = 2$ is very close to the diffusivity given by the BC model for the same value of λ. Varying the parameter c in the vicinity of 2, one can obtain very good agreement between these two models for $\Theta < 0.8$. However for large values of $\Theta > 0.8$, the MvG model is preferable, as was mentioned above. The SF model in contrast to the BC model approximates well the diffusivity function for large values of $\Theta > 0.5$.

We shall focus on one-dimensional processes when the liquid percolates into a porous medium as an homogeneous plane wave moving either vertically downward from the surface towards the bulk of medium or horizontally. The first problem is called infiltration and will be treated further as a problem of water propagation under the influence of gravity. The second problem is called the imbibition, as suggested by R.E. Smith [10] and describes liquid percolation in the horizontal direction without the influence of gravity force.

In one-dimensional case Eq. (9) has the form

$$\frac{\partial \theta}{\partial t} = \frac{\partial}{\partial x}\left[D(\theta)\frac{\partial \theta}{\partial x} - sK(\theta)\right] \tag{14}$$

or equivalently in terms of function Θ (see Eq. (4))

$$\frac{\partial \Theta}{\partial t} = \frac{\partial}{\partial x}\left[D(\Theta)\frac{\partial \Theta}{\partial x} - \frac{s}{\theta_s - \theta_r}K(\Theta)\right], \tag{15}$$

where the formal parameter s was inserted to switch easily from the imbibition problem ($s = 0$) to the infiltration problem ($s = 1$). For the infiltration problem the spatial variable x is a vertical coordinate while for the imbibition problem it is a horizontal coordinate.

3 Self-similar front solutions of the Richards' equation

Let us seek self-similar solutions to Eq. (15) in the form

$$\Theta(t, x) = t^{\alpha}\Phi(\xi), \quad \xi = xt^{\beta}, \tag{16}$$

where α and β are some unknown exponents to be determined [1]. Equation (15) in the new variables can be rewritten as

$$\alpha\Phi + \beta\xi\frac{d\Phi}{d\xi} = t^{2\beta+1}\frac{d}{d\xi}\left[D\left(t^{\alpha}\Phi\right)\frac{d\Phi}{d\xi} - \frac{s}{\theta_s - \theta_r}t^{-(\alpha+\beta)}K\left(t^{\alpha}\Phi\right)\right]. \qquad (17)$$

According to the general theory of self-similar solutions [1], exponents α and β should be chosen so that the resultant equation (17) does not depend on t and depends only on the self-similar variable ξ.

3.1 Self-similar solutions of the first kind

The only possibility for Eq. (17) to be independent of t given arbitrary functions $D(\Theta)$ and $K(\Theta)$ is to have $s = 0$, ie be in the imbibition case. Then one has the solution $\alpha = 0$ and $\beta = -1/2$. Eq. (17) then reduces to

$$\frac{d}{d\xi}\left[D(\Phi)\frac{d\Phi}{d\xi}\right] + \frac{\xi}{2}\frac{d\Phi}{d\xi} = 0. \qquad (18)$$

The corresponding self-similar solution in the form of a step-wise function was obtained numerically by Philip [6] (see also [10]). The solution $\Theta(t, x) = \Phi(x/\sqrt{t})$ represents the diffusion of a liquid in a porous medium without gravity between two asymptotically constant values, Θ_1 at plus infinity and Θ_2 at minus infinity. The limiting values may be any constants in the range $0 \leq \Theta_1, \Theta_2 \leq 1$.

A similar solution can be obtained for other models of the retention function. It is of interest to compare the structures of self-similar step-wise solutions for the two limiting cases of small and large liquid saturation where the applicable models are BC and SF, respectively. The corresponding equations are:

$$\text{BC model:} \qquad \frac{d^2\Phi^{3+1/\lambda}}{d\xi^2} + \frac{3 + 1/\lambda}{2D_0}\xi\frac{d\Phi}{d\xi} = 0; \qquad (19)$$

$$\text{SF model:} \qquad \frac{d^2}{d\xi^2}\frac{1}{b - \Phi} + \frac{1}{2D_0 a}\xi\frac{d\Phi}{d\xi} = 0. \qquad (20)$$

For the front solutions, the following boundary conditions were assumed: $\Phi(\xi = -\infty) = \Phi_l$, $\Phi(\xi = +\infty) = \Phi_r$. Because of the structure of the system, these conditions imply $d\Phi/d\xi = 0$ for $\xi \to \pm\infty$. For the calculation, the boundary values Φ_l and Φ_r were prescribed at some large finite values of ξ.

To solve this boundary value problem numerically we used the Matlab bvp4c solver [11] based on collocation. The results obtained are shown in Fig. 4. The panel labeled (a) shows the front for the BC model. Note how the fronts get wider as the difference $\Theta_l - \Theta_r$ increases. They get very steep so that up to 30000 collocation points were needed for a relative tolerance 10^{-4}. For the SF model shown in panel (b), the fronts seem to have a constant width and they are smoother.

3.2 Self-similar solutions of the second kind

When the functions $D(\Theta)$ and $K(\Theta)$ in Eq. (15) are of power type, i.e., they are self-similar themselves, one can remove the dependency on t in Eq. (17). This is the case for the BC model. Substituting the $D(\Theta)$ and $K(\Theta)$ functions of the BC-model Eq. (10) and (6) into Eq. (17) one can reduce this equation to the following form

$$\alpha\Phi + \beta\xi\frac{d\Phi}{d\xi} = t^{2\beta+1+2\alpha+\alpha/\lambda}\Phi^{2+1/\lambda}\frac{d}{d\xi}\left[D_0\frac{d\Phi}{d\xi} - \frac{sK_s^{3+2/\lambda}}{\theta_s-\theta_r}t^{\alpha/\lambda-\beta}\Phi^{1+1/\lambda}\right]. \tag{21}$$

This equation is independent on t if the exponents α and β are

$$\alpha = -\frac{\lambda}{3+2\lambda}, \qquad \beta = -\frac{1}{3+2\lambda}. \tag{22}$$

Since $\alpha < 0$ this solution gradually decays with time as follows from Eq. (16), $\Theta(t,x) \sim t^{-\frac{\lambda}{3+2\lambda}}$. Such behavior is meaningful for a pulse-type solution rather than for a front-type because a uniform time decay of a constant liquid content at different asymptotics is unlikely from the physical point of view. A consequence of Eq. (15) is that for pulse-type solutions there is a "mass" conservation integral:

$$M = \int_{-\infty}^{\infty} \Theta(t,x)\,dx = \text{const}. \tag{23}$$

(this integral does not make sense for front-type solutions since it is infinite in that case). Substituting the solution (16) into this equation yields

$$\int_{-\infty}^{\infty} \Theta(t,x)\,dx = t^{\alpha}\int_{-\infty}^{\infty} \Phi(xt^{\beta})\,dx = t^{\alpha-\beta}\int_{-\infty}^{\infty} \Phi(\xi)\,d\xi = \text{const}. \tag{24}$$

This condition can be satisfied only if $\alpha = \beta$, which is possible when $\lambda = 1$. With this value of λ and defining the new independent variable $\chi = \xi/\sqrt{D_0}$, Eq. (21) finally reads:

$$5\Phi^3\frac{d^2\Phi}{d\chi^2} + \frac{d}{d\chi}\left(\chi\Phi - \frac{s}{\sqrt{D_0}}\frac{K_s^5}{\theta_s - \theta_r}\Phi^5\right) = 0. \tag{25}$$

For the imbibition problem, $s = 0$, this equation further simplifies:

$$5\Phi^3\frac{d^2\Phi}{d\chi^2} + \frac{d}{d\chi}\left(\chi\Phi\right) = 0. \tag{26}$$

Numerical solutions to this equation are shown in Fig. 5a for three values of the parameter A_0 which determines the function maximum. This parameter is directly linked to the total "mass" of the solution M and depends on the amount of liquid injected into the soil at a certain location. Equation (26) is invariant with respect to the transformation $\chi \to -\chi$ and its solutions are symmetric with respect to the vertical axis. The asymptotics at 0 and ∞ of such solutions can be readily calculated, they are:

$$\Phi(\chi) \approx a_0 - \frac{\chi^2}{10a_0^2} + \frac{\chi^6}{5000a_0^8} + \frac{9\chi^8}{350000a_0^{11}} + \frac{23\chi^{10}}{10500000a_0^{14}} + \ldots; \tag{27}$$

$$\Phi(\chi) \approx \frac{b_{-1}}{\chi} + \frac{2b_{-1}^4}{\chi^6} + \frac{48b_{-1}^7}{\chi^{11}} + \ldots \tag{28}$$

As usually happens with self-similar solutions of this sort (see, [1]), the solution in terms of $\Theta(t, \xi)$, Eq. (16) diverges when $t \to 0$. Actually, the self-solution makes sense in the asymptotic, when t is large enough and function $\Theta(t, \xi)$ describing liquid content in the soil becomes less than 1.

For the infiltration problem, $s = 1$, changing the variables in Eq. (21):

$$\chi = \frac{\xi K_s^3}{D_0^{4/5}(\theta_s - \theta_r)^{3/5}}, \quad \Psi = \frac{\Phi K_s^2}{D_0^{1/5}(\theta_s - \theta_r)^{2/5}} \tag{29}$$

leads to the equation (one should bear in mind that $\alpha = \beta = -1/5$ and $\lambda = 1$):

$$5\Psi^3\frac{d^2\Psi}{d\chi^2} - 10\Psi^4\frac{d\Psi}{d\chi} + \frac{d\left(\chi\Psi\right)}{d\chi} = 0. \tag{30}$$

Numerical solutions to this equation are shown in Fig. 5b for the same three values of the parameter A_0 as in Fig. 5a. The asymptotics of these solutions

are:

$$\Psi(\chi) \approx a_0 - \frac{\chi^2}{10a_0^2} - \frac{\chi^3}{15a_0} - \frac{\chi^4}{30} + \frac{1-5a_0^5}{375a_0^4}\chi^5 + \ldots; \quad (31)$$

$$\Psi(\chi) \approx \frac{b_{-1}}{\chi} + \frac{2b_{-1}^4(1+b_1)}{\chi^6} + \frac{4b_{-1}^7(12+17b_{-1}+5b_{-1}^2)}{\chi^{11}} + \ldots \quad (32)$$

In terms of the physical variable $\Theta(\xi, t)$ the liquid content in the medium both for the imbibition and infiltration problems slowly decays with time $\Theta(\xi, t) \sim t^{-1/5}$, and the characteristic size of the domain occupied by the liquid, Λ, gradually increases, $\Lambda \sim t^{1/5}$.

4 Travelling front solutions of the Richards' equation

Consider now travelling wave solutions of Eq. (15) in the form $\Theta(t, x) = \Theta(x - Vt) \equiv \Theta(\zeta)$, where V is the velocity of the stationary wave. Note that travelling wave solutions can be also treated as self-similar solutions [1]. Indeed, making a transformation $t = \log\tau$ and $x = \log\chi$ the above solution can be presented in the form $\Theta(\tau, \chi) = \Theta\left[\log\left(\chi\tau^{-V}\right)\right]$. We use however the traditional approach. For such solutions Eq. (15) may be integrated once resulting in

$$\frac{d\Theta}{d\zeta} = \frac{s}{\theta_s - \theta_r}\frac{K(\Theta)}{D(\Theta)} + \frac{C - V\Theta}{D(\Theta)}, \quad (33)$$

where C is a constant of integration. The value of this constant as well as the wave velocity V can be determined from the boundary conditions. Assuming that the solution has the form of a shock wave with constant values at plus and minus infinity, $\Theta(\infty) = \Theta_1, \quad \Theta(-\infty) = \Theta_2$ $(0 \le \Theta_1,\ \Theta_2 \le 1)$ and $\frac{d\Theta}{d\zeta} = 0$ at $x = \pm\infty$, one can readily find

$$V = \frac{s}{\theta_s - \theta_r}\frac{K(\Theta_2) - K(\Theta_1)}{\Theta_2 - \Theta_1}, \quad (34)$$

$$C = \frac{s}{\theta_s - \theta_r}\frac{\Theta_1 K(\Theta_2) - \Theta_2 K(\Theta_1)}{\Theta_2 - \Theta_1} \quad (35)$$

This travelling wave solution corresponds to the heteroclinic orbit connecting the two fixed points $\Theta = \Theta_1$ and $\Theta = \Theta_2$ on the phase plane $(\Theta',\ \Theta)$ where

$\Theta' \equiv \frac{d\Theta}{d\zeta}$. Note that both constants V and C are independent of the diffusivity function $D(\Theta)$, they only depend on the convection function $K(\Theta)$. On the other hand the profile of the water front does depend on $D(\Theta)$. Also note that from these equations, both constants V and C are formally zero if $s = 0$, i.e., for the imbibition problem. In this case Eq. (33) is degenerate and must be reconsidered separately for the shock wave solutions.

4.1 Steady-state solutions of the imbibition problem

For this particular case, Eq. (33) reduces to

$$\frac{d\Theta}{d\zeta} = \frac{C - V\Theta}{D(\Theta)}. \tag{36}$$

Solutions to this equation can be analyzed by means of the phase plane. For the BC model this equation takes the form:

$$\Theta' = \frac{C_1 - \Theta}{\Theta^{2+\frac{1}{\lambda}}}, \tag{37}$$

where $C_1 = C/V$. It is easy to see that for $0 < C_1 < 1$, there is a fixed point of this equation, $\Theta = C_1$ and it is the only one (we recall that the variable Θ has a physical meaning only within the interval $0 \le \Theta \le 1$). Therefore no front solution exists for this model.

For the other models, MvG and SF, it is possible to get another fixed point Θ_2 which corresponds to $D(\Theta_2) = \infty$. In particular, for the MvG model Eq. (33) reduces to

$$\Theta' = \frac{(C_1 - \Theta)\Theta^{1/\lambda+1/2}}{\left[1 - \left(1 - \Theta^{c/\lambda}\right)^{\lambda/c}\right]^2 \left(1 - \Theta^{c/\lambda}\right)^{1/c-1}}. \tag{38}$$

This equation can have two stationary points in the physical range of the variable Θ. The first point is the same as above, i.e., $\Theta = C_1$ if $0 < C_1 < 1$, and the second point is $\Theta = 1$ if parameter $c > 1$. This difference between equations (37) and (38) is not surprising because, as was mentioned above, the BC model does not work correctly in the vicinity of the point $\Theta = 1$. The phase portrait of Eq. (38) is shown in Fig. 6a.

The SF model, contrarily to the BC model, is mainly applicable in the vicinity of the point $\Theta = 1$ and is unapplicable for $\Theta < 0.5$. Hence, one can

expect that it gives qualitatively the same results as the MvG model. The corresponding equation is much simpler for this case:

$$\Theta' = \frac{(C_1 - \Theta)(b - \Theta)^2}{a}. \tag{39}$$

The phase portrait of this equation is shown in Fig. 6b. For this case the analytical solution describing the shock-wave profile can be obtained in the implicit form:

$$x - x_0 = \frac{a}{(b - C_1)^2}\left(\ln\frac{b - \Theta}{\Theta - C_1} - \frac{b - C_1}{b - \Theta}\right). \tag{40}$$

Figure 7 illustrates shock-wave profiles for three values of constant C_1. The peculiarity of these solutions is that the limiting value of variable Θ at the minus infinity, $\Theta(-\infty) = b \approx 1$ that means that the soil is completely liquid saturated there. The other asymptotic value at the plus infinity can be arbitrary, $\Theta(\infty) = C_1 \equiv C/V$. Thus, a steady-state shock-wave solution can exist for the imbibition problem only when at minus infinity the soil is completely saturated.

The wave profile is almost antisymmetrical with respect to its midpoint when the difference in soil saturations at plus and minus infinities are close to each other. Otherwise the profile is asymmetrical (compare, e.g., the wave profiles shown in Fig. 6 for $C_1 = 0.9$ and $C_1 = 0.7$). The wave velocity V and front thickness $d \equiv |D_0|/V$ remain undefined even for the given limiting values of shock asymptotics, $\Theta(-\infty) = 1$ and $\Theta(\infty) = C_1$. Note that the water front profile for small C_1 qualitatively agrees with that described by the self-similar solution presented in [10] and in Fig. 4.

4.2 Steady-state solutions of the infiltration problem

Let us consider now the infiltration problem in the vertical direction. The governing equation for steady-state waves is Eq. (33) with $s = 1$. The substitution of expressions (34) and (35) for V and C into Eq. (33) yields

$$\frac{d\Theta}{d\zeta} = \frac{1}{(\theta_s - \theta_r)D(\Theta)}\left[K(\Theta) - \frac{K(\Theta_2) - K(\Theta_1)}{\Theta_2 - \Theta_1}\Theta + \frac{\Theta_1 K(\Theta_2) - \Theta_2 K(\Theta_1)}{\Theta_2 - \Theta_1}\right]. \tag{41}$$

This equation has shock-type solutions for any values of the variable Θ at plus and minus infinities within the range $0 \le \Theta_1, \Theta_2 \le 1$. These limiting values, Θ_1 and Θ_2, determine the velocity of the moving front in accordance with Eq. (34).

Let us consider the phase plane of this equation for two limiting cases, the BC and SF models, which are relatively simple for the analysis. Substituting the corresponding functions $D(\Theta)$ and $K(\Theta)$ into equation (34), one obtains the phase portraits for the BC and SF models shown in Fig. 8. Phase trajectories are not symmetric and do not follow the parabolic shape that is typical for the Burgers equation [14] (for this equation $K(\Theta) = \Theta^2$). As one can see from Fig. 8a, the quadratic approximation of the nonlinear function in the right-hand side of Eq. (41) is appropriate only for very close located fixed points when $(\Theta_2 - \Theta_1)/\Theta_1 \ll 1$. However, qualitatively the shock-wave profiles of Eq. (41) are similar to the classical Burgers solutions. They are shown in Fig. 9.

Shock-wave solutions correspond to the heteroclinic orbit connecting the points $(\Theta_1, 0)$ and $(\Theta_2, 0)$ in the phase plane. One can compute such orbits by solving the ordinary differential equation (41) with an initial condition which is very close, e.g., to $(\Theta_2, 0)$. Because of the local existence and uniqueness of the solution, the representative point evolves to $(\Theta_1, 0)$. Such solutions correspond to the moving moisture fronts downward from the wet towards the relatively dry soil.

5 Stability of front solutions of the Richards' equation

In this section we examine numerically the stability of the self-similar and travelling front solutions that we found in the previous sections. To do this we solve the Richards partial differential equation (15) numerically. As a first step it is convenient to rewrite it in the form of a conservation law and integrate it then on small intervals on which the solution is assumed to be constant. This is in the spirit of the finite volume method; more details are given in the Appendix. Richards' equation (15) was solved on a very large domain whose length $2l$ is much greater than the characteristic front size d ($l \sim 10^3 \cdot d$). Dirichlet boundary conditions $\Theta(x = -\infty) = \Theta_l$ and $\Theta(x = \infty) = \Theta_r$ were used. The initial condition was chosen in the form

$$\Theta(x, t = 0) = \Theta_l - \frac{\Theta_l - \Theta_r}{2} \left(1 + \tanh \frac{x - x_0}{w_0}\right), \tag{42}$$

where w_0 is the width of the front.

For the infiltration problem our calculations show that numerical solutions always relaxed to the steady-state travelling front solution given by Eq. (41). Figure 10 presents $\Theta(x,t)$ as a function of the normalized coordinate $\zeta = \frac{K_s}{D_0(\theta_s-\theta_r)}x$ for the BC model with a typical initial condition $\Theta_2 = 0.8$, $\Theta_1 = 0.1$ and $w_0 = 2$ at successive times from $t = 0$ to $t = 80$. As one can see, the perturbation front sharpens and quickly stabilizes to the steady-state profile which is also shown in the figure (the line labelled "Analyt"). In accordance with the theoretical prediction, the profile is not symmetrical; it has a smoothed edge at the top and almost right-angle edge at the bottom. The front velocity determined from the numerical data $V_n \approx 0.47$ agrees well with the theoretical value for this case $V_t = 0.468$.

The stability of the front profile was confirmed for all the other values of Θ_1 and Θ_2 that were investigated and also for soil retention functions different from the Brooks and Corey model. As an example, Fig. 11 shows the formation of steady-state profiles from an initial step-wise perturbation for the MvG model with different values of Θ_2. Again the front velocity obtained numerically agrees well with the theoretical values and as expected it increases when $|\Theta_2 - \Theta_1|$ increases. For the case shown in Fig. 11a), $V_n \approx 0.189$, whereas $V_t = 0.187$; for the case shown in Fig. 11b), $V_n \approx 0.436$, whereas $V_t = 0.434$ and for the case shown in Fig. 11c), $V_n \approx 0.815$, whereas $V_t = 0.813$. Front profiles look more symmetrical for the MvG model than for the BC model, especially when Θ_2 is closer to Θ_1 (cf. Fig. 11 with Fig. 9a). For the same limiting values of liquid saturation, the MvG model provides smoother and wider shock-wave profiles than the BC model.

For the imbibition problem there is no convective term in the Richards equation (15) due to $s = 0$. The equation is then a nonlinear diffusion equation. Figure 12a shows the typical evolution of the initial condition (42) as a function of x for six successive times for the SF model. The boundary values are $\Theta_2 = 0.9$ and $\Theta_1 = 0.75$. As expected, the front does not translate and its width increases continuously with time. When these profiles are plotted against the self-similar variable $\xi = (x - 200)/\sqrt{t}$, all plots reduce to a single one. This is shown in Fig. 12b. This plot is in excellent agreement with the self-similar

solution of the first kind obtained in subsection 3.1. Similar results have been obtained for the BC and MvG models so this seems to be a general result.

6 Conclusion

We analyzed and studied numerically water front propagation in a soil both with and without the effect of gravity. The corresponding infiltration and imbibition problems are described by the Richards' convection-diffusion equation. Three different analytical approximations of the soil retention function, the Brooks–Corey, the Mualem–Van Genuchten and the Storm–Fujita models were examined and the results obtained were compared.

For the infiltration problem we showed that front solutions always exist. Their speeds were calculated and their stability was proven numerically. All soil models show stability of the moving wetting fronts. This seems to be a general result for the monotonic dependency of soil conductivity $K(\Theta)$.

For the imbibition problem the self-similar front solutions were found for all soil models as functions of the reduced variable $x/\sqrt{t}$. The results obtained were compared with the known Philip's solution [6, 10]. In all numerically studied cases it was observed that any initial profile between two constant values Θ_2 and Θ_1 tends eventually to the self-similar front indicating its stability.

In addition to that, pulse-type self-similar solution of the second kind was discovered for the BC model both for the imbibition and infiltration cases. Such solution can be treated as an intermediate asymptotic [1] for the localized initial perturbations occupying a finite domain, e.g., wetted soil layer located at certain depth initially and then, diffusing either horizontally or vertically.

The results on travelling and self-similar fronts are important for fundamental science as well as applications because Richards' equation is a generalization of Burgers equation. The results are also highly relevant for soil physics because they allow one to estimate the time for a soil to reach a certain water content. This time is given by the slope of the conductivity profile for the infiltration problem. For the imbibition case the time is given by the diffusion constant and can be easily estimated.

Acknowledgments. The authors are thankful to D. Stone for his interest to this work and permanent support. J.-G. C. is grateful for the invitation from ANSTO, Australia where this work was initiated, and appreciative of the hospitality during his visit in June 2003. Y.A.S. is grateful for the invitation from the Université de Cergy-Pontoise and INSA de Rouen, France and appreciative of the hospitality during his visit in September 2003.

References

[1] Barenblatt G.I. *Scaling, Self-similarity, and Intermediate Asymptotics*. Cambridge University Press, 1996, 386 p.

[2] Buckingham E. Studies on the movement of soil moisture. *U.S. Dept. of Agriculture Bureau of Soils Bull.*, 1907, **38**.

[3] Fujita H. The exact pattern of a concentration-dependent diffusion in a semi-infinite medium. 2. *Textile Res. J.*, 1952, **22**, 823–827.

[4] Mualem Y. A new model for predicting the hydraulic conductivity of unsaturated porous media. *Water Resources Res.*, 1976, **12**, 513–522.

[5] Pantelis G., Ritchie A.I.M., Stepanyants Y.A. A conceptual model for the description of oxidation and transport processes in sulfidic waste rock dumps. *Appl. Math. Model.*, 2002, **26**, n. 6, 751–770.

[6] Philip J.R. Theory of infiltration, in *Advances in Hydroscience*, V. 5, ed. V. T. Chow, Academic Press, N.Y., 1969, 215–296.

[7] Richards L.A. Capillary conduction of liquids through porous mediums. *Physics*, 1931, **1**, 318–333.

[8] Rogers C., Stallybrass M.P., Clements D.L. On two phase filtration under gravity and with boundary infiltration: Application of a Bäclund transformation. *Nonlinear Anal. Theory Methods Appl.*, 1983, **7**, 785–799.

[9] Scott A. C. (Ed.) *Encyclopedia of Nonlinear Science*, Routledge, New York and London, 2005, 1053 p.

[10] Smith R.E. *Infiltration Theory for Hydrologic Applications*, AGU, Washington, 2002, 212 p.

[11] The Mathworks, Inc.
www.mathworks.com

[12] Storm M.L. Heat conduction in simple metals. *J. Appl. Phys.*, 1951, **22**, 940–951.

[13] Van Genuchten M.Th. A closed-form equation for predicting the hydraulic conductivity of unsaturated soils. *Soil Science Soc. of America J.*, 1980, **44**, (5), 892–898.

[14] Whitham G.B. *Linear and Nonlinear Waves.* – J. Wiley & Sons, 1974, 636 p.

7 Appendix: Numerical procedure for solving 1D Richards' equation

To integrate numerically 1D Richards' equation we write it as a conservation law.

$$\frac{\partial \Theta}{\partial t} = \frac{\partial}{\partial x}\left[D(\Theta)\frac{\partial \Theta}{\partial x} - \frac{s}{\theta_s - \theta_r}K(\Theta)\right], \tag{43}$$

which we integrate over reference intervals in space following the finite volume procedure. We assume the solution to be constant on those intervals and equal to the value at the center of interval. The time advance is done with a Runge–Kutta 4-5 ordinary differential equation solver. We assume Dirichlet boundary conditions on the edges of the numerical domain $[-l, l]$ so that $\Theta(x = -l, t) = \Theta_l$ and $\Theta(x = l, t) = \Theta_r$.

The resulting discrete equations for a given node n center of a reference interval are

$$h\dot{\Theta}_n = \Big[D(\Theta)\Theta_x - K(\Theta)\Big]_{x_n - h/2}^{x_n + h/2}$$

$$\approx D\left(\frac{\Theta_{n+1} + \Theta_n}{2}\right)\frac{\Theta_{n+1} - \Theta_n}{h} - D\left(\frac{\Theta_n + \Theta_{n-1}}{2}\right)\frac{\Theta_n - \Theta_{n-1}}{h}$$

$$-\frac{s}{\theta_s-\theta_r}\left[K\left(\frac{\Theta_{n+1}+\Theta_n}{2}\right)+K\left(\frac{\Theta_n+\Theta_{n-1}}{2}\right)\right]. \tag{44}$$

The numerical scheme is stable for $\delta t/h^2 < 1$, typically we have chosen $2l = 300$ and $h = 0.3$. The time step is chosen to that the tolerance for the truncation error is smaller than 10^{-5} so that $\delta t < 0.1$.

We have first tested this scheme against Burgers equation for which $D(\Theta) \equiv D$ just a constant, and $K(\Theta) \equiv \Theta^2$. Numerical results were compared with the exact solution describing shock wave propagation [14]. With the indicated values of $D(\Theta)$ and $K(\Theta)$, Richards' equation reduces to the following Burgers equation

$$\Theta_t = \Theta\Theta_x + D\Theta_{xx}, \tag{45}$$

which can be transformed by means of Hopf–Cole transformation $\Theta = -2D\phi_x/\phi$ to the usual heat equation for function ϕ [14]

$$\phi_t = D\phi_{xx}. \tag{46}$$

Elementary solution of this equation $\phi = 1+e^{kx-\omega t}$ gives the two parametric shock solution of Burgers equation:

$$\Theta_s(x,t) = -2Dk\frac{e^{k(x-x_0)-Dk^2t}}{1+e^{k(x-x_0)-Dk^2t}}, \tag{47}$$

which separates a region where $\Theta = 0$ for $x = -\infty$ from the region where $\Theta = -2Dk$ for $x = +\infty$ and moves with the velocity $V_{sh} \equiv \omega/k = Dk$. A characteristic shock thickness is $1/k$.

It has been tested and verified that any stepwise initial condition between $\Theta = 0$ and $\Theta = \Theta_r$ tends to the shock-type travelling wave solution mowing with the corresponding velocity $V_{sh} = -\Theta_r/2$.

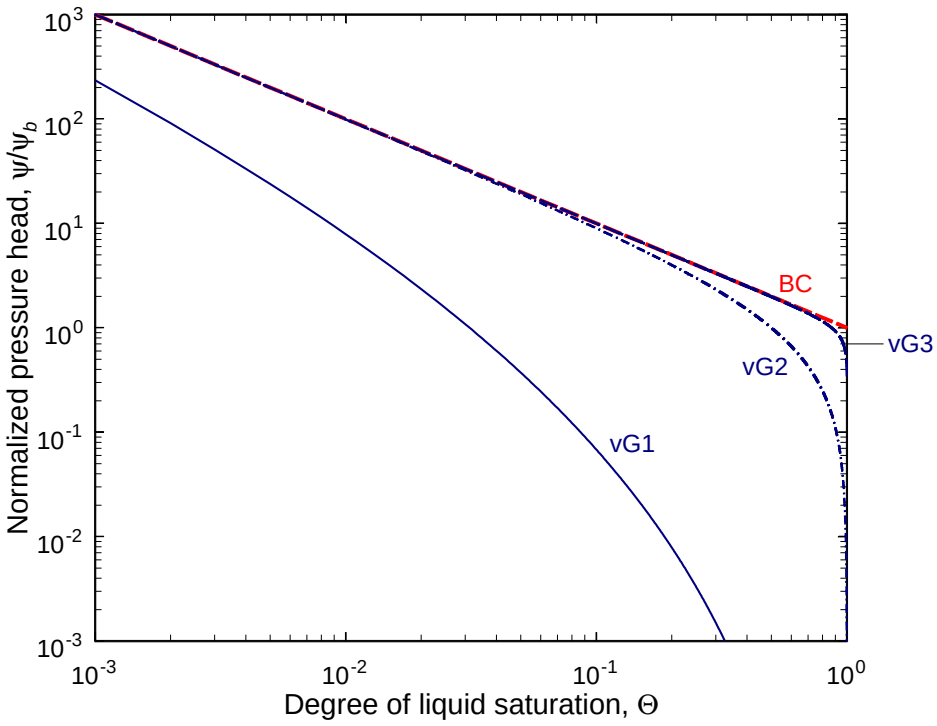

Figure 1: Plot of the normalized pressure head, ψ/ψ_b vs the degree of liquid saturation in a porous medium, Θ, for the BC model with $\lambda = 1.0$, and the vG model with the same λ and different values of c: curve vG1 – $c = 0.5$; curve vG2 – $c = 1$ and curve vG3 – $c = 2$.

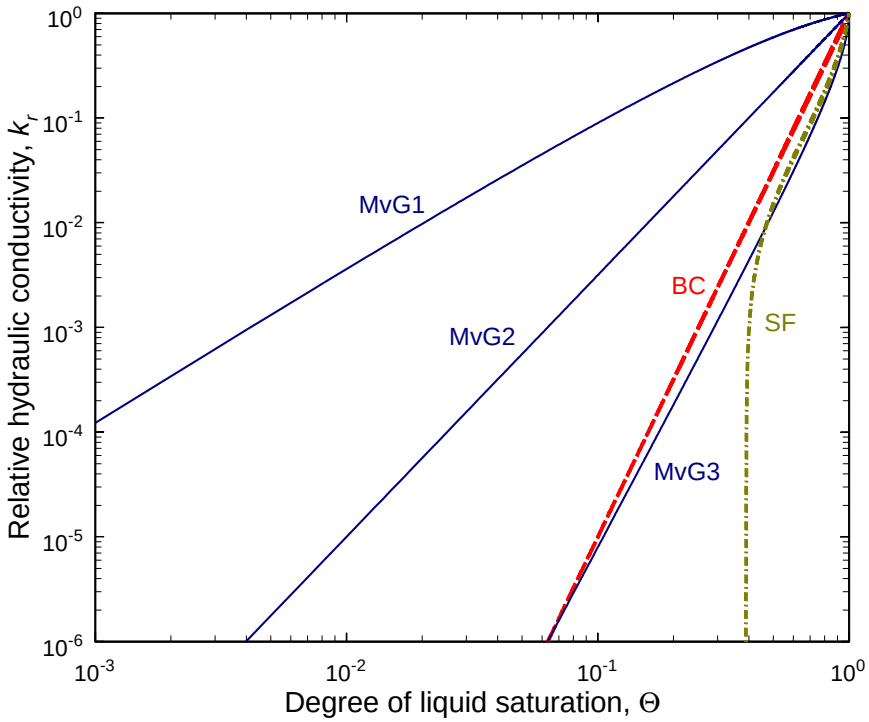

Figure 2: Plot of the relative hydraulic conductivity, k_r, vs the degree of liquid saturation in a porous medium, Θ, for the BC model with $\lambda = 1.0$, MvG model with the same value of λ and different c: curve MvG1 – $c = 0.5$; curve MvG2 – $c = 1$ and curve MvG3 – $c = 2$, and SF model with $\Lambda = 0.128$ and $E = 0.1$.

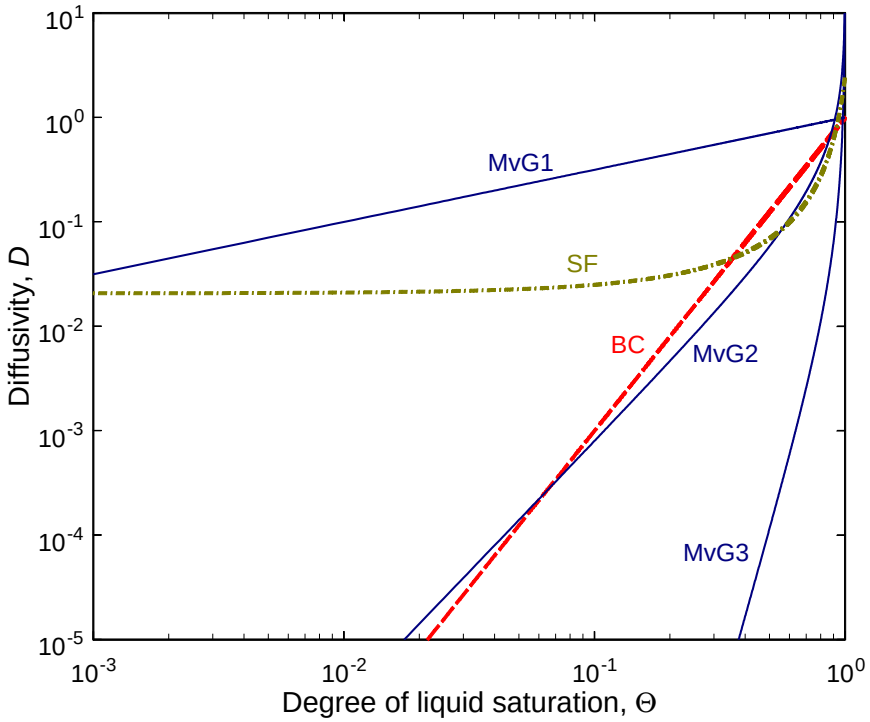

Figure 3: Plot of the normalized diffusivity, D/D_0, vs the degree of liquid saturation in a porous medium, Θ for the BC model (straight line) with $\lambda = 1.0$, the MvG model with the same λ and different values of c: straight line MvG1 – $c = 1$; line MvG2 – $c = 2$ and line MvG3 – $c = 5$, and the SF model with $a = 0.025$ and $b = 1.1$.

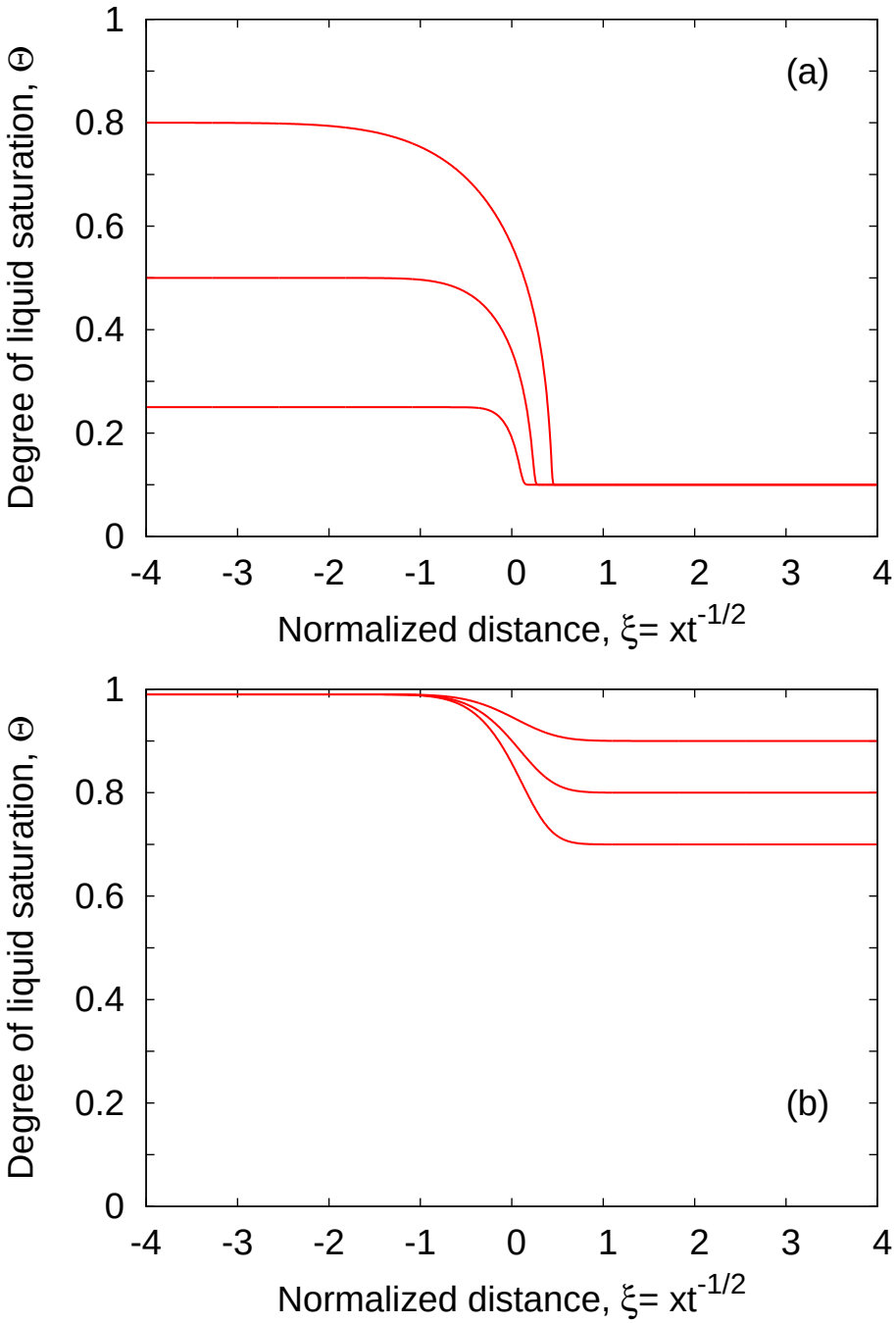

Figure 4: Front-type self-similar solutions for the imbibition problem for two different soil models: a) – BC model with $\lambda = 1$, b) – SF model with $b = 1.5$, $a = 0.025$. In each plot three different couples (Θ_l, Θ_r) are shown. The parameter $D_0 = 1$

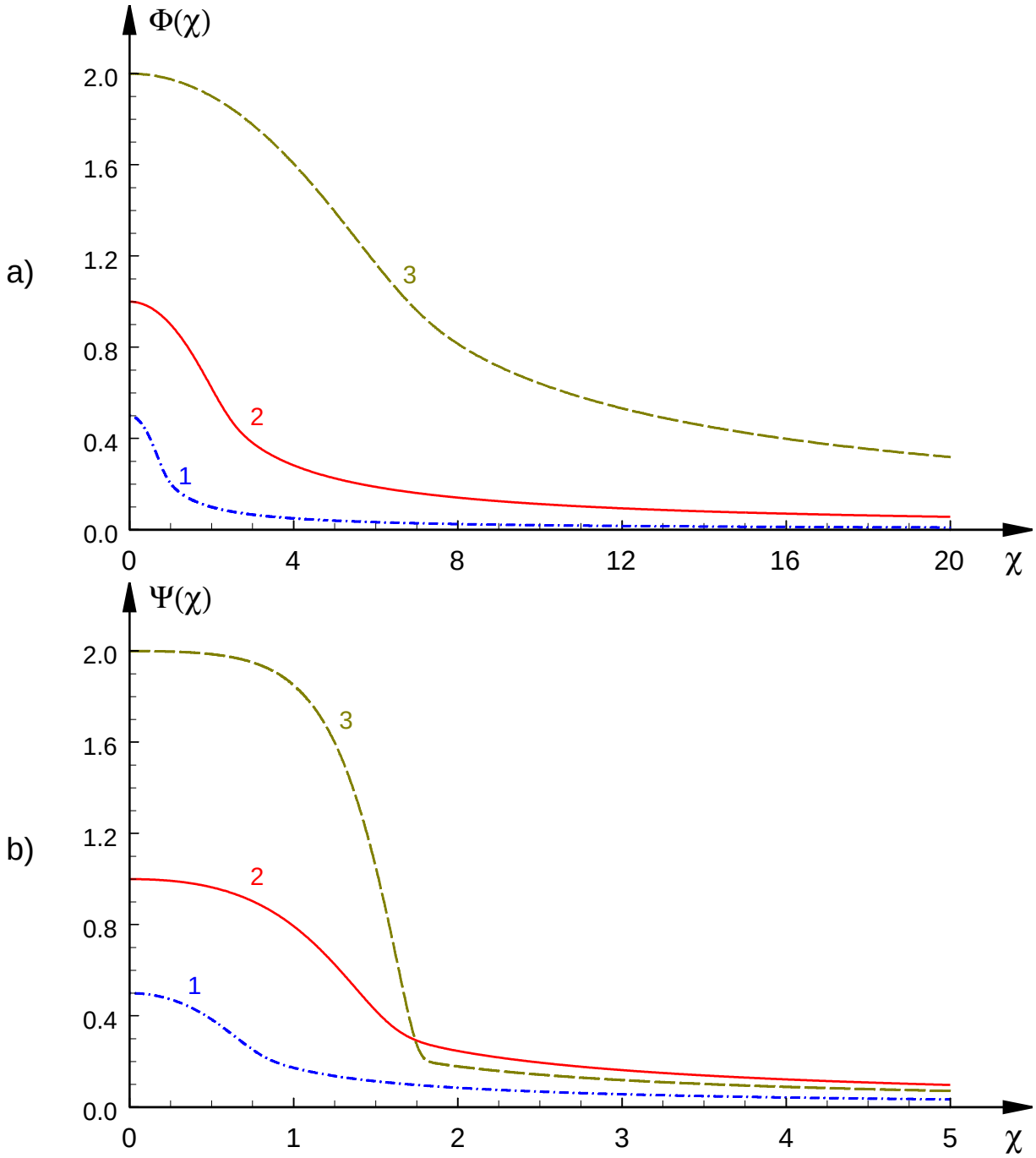

Figure 5: Self-similar solutions of the second kind for the BC model with $\lambda = 1$ (only the right-halves of symmetric functions are shown). a) Imbibition problem; b) infiltration problem (the horizontal scale is four times stretched). Different lines correspond to different amplitudes of the functions Φ and Ψ: $1 - A_0 = 0.5$, $2 - A_0 = 1.0$, $3 - A_0 = 2.0$.

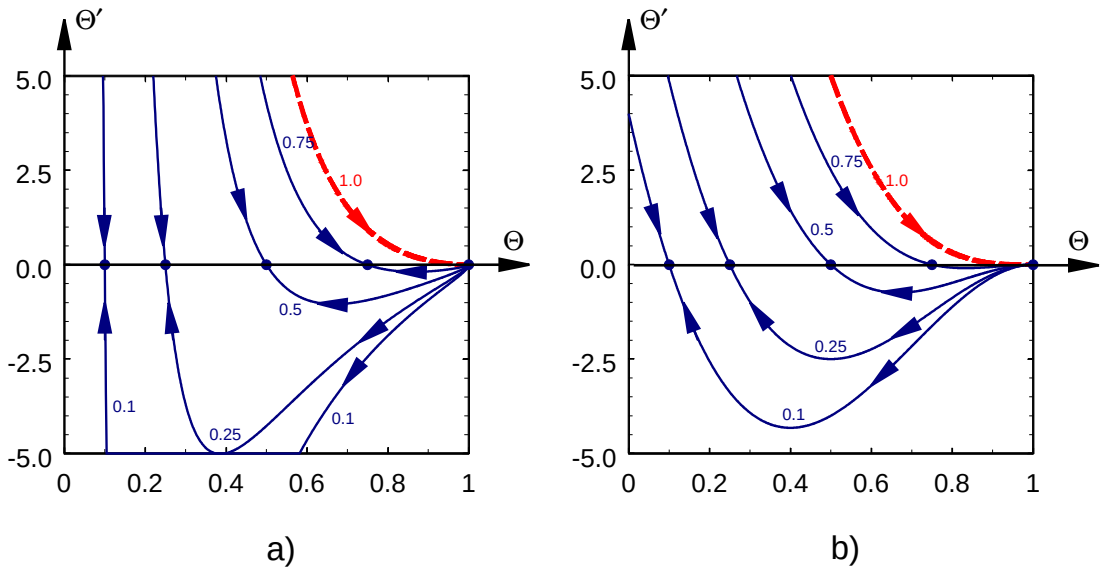

Figure 6: Phase portraits for the travelling wave ODEs for the imbibition problem: a) – Eq. (38) with $c = 2$ (MvG model) and b) – Eq. (39) with $a = 0.025$ and $b = 1$ (SF model). The dots indicate the equilibrium positions ($\Theta = C_1, \Theta' = 0$) for different values of the constant C_1. The corresponding orbits are labelled with C_1.

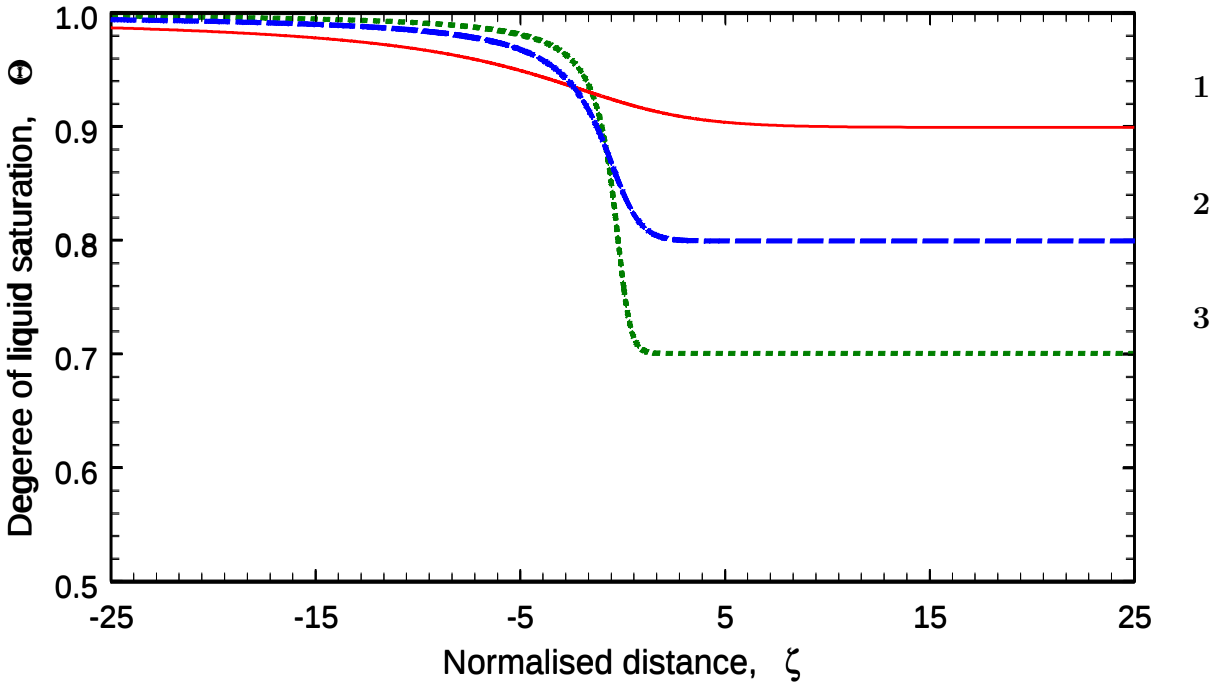

Figure 7: Travelling wave solutions for the imbibition problem given by Eq. (36) for the SF model and three values of the constant $C_1 = 0.9$ (line 1), 0.8 (line 2) and 0.7 (line 3). Other parameters are $a = 0.025, b = 1$.

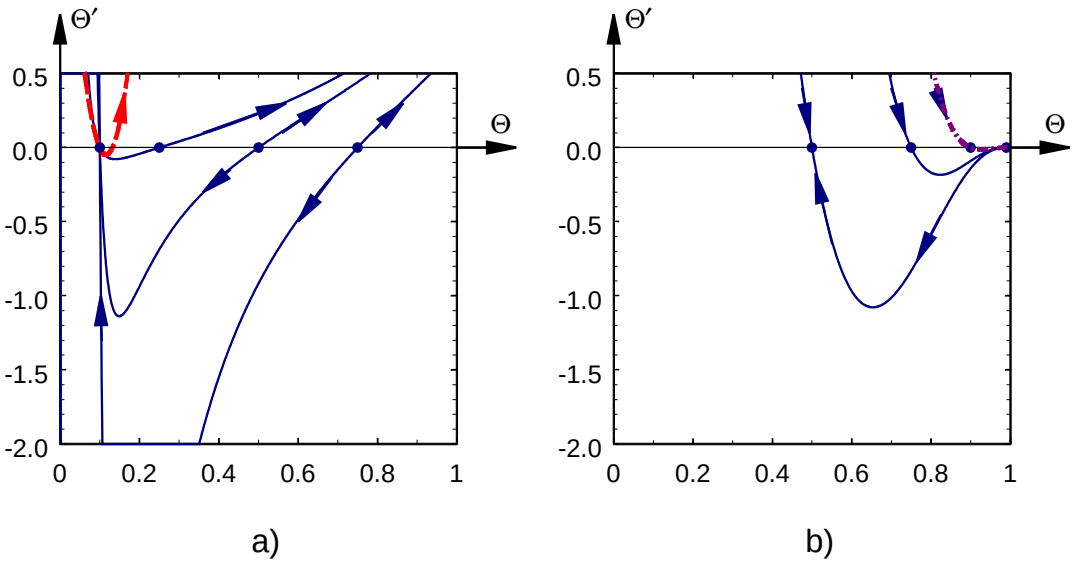

Figure 8: a) The phase portrait of Eq. (41) for the BC model. One equilibrium point, $\Theta_1 = 0.1$, is fixed for simplicity and another one, Θ_2, varies. The parabolic dashed line corresponds to the Burgers model. b) Phase-portrait for the SF model. Now the equilibrium point $\Theta_2 = 1$ is fixed and another equilibrium point, Θ_1, varies.

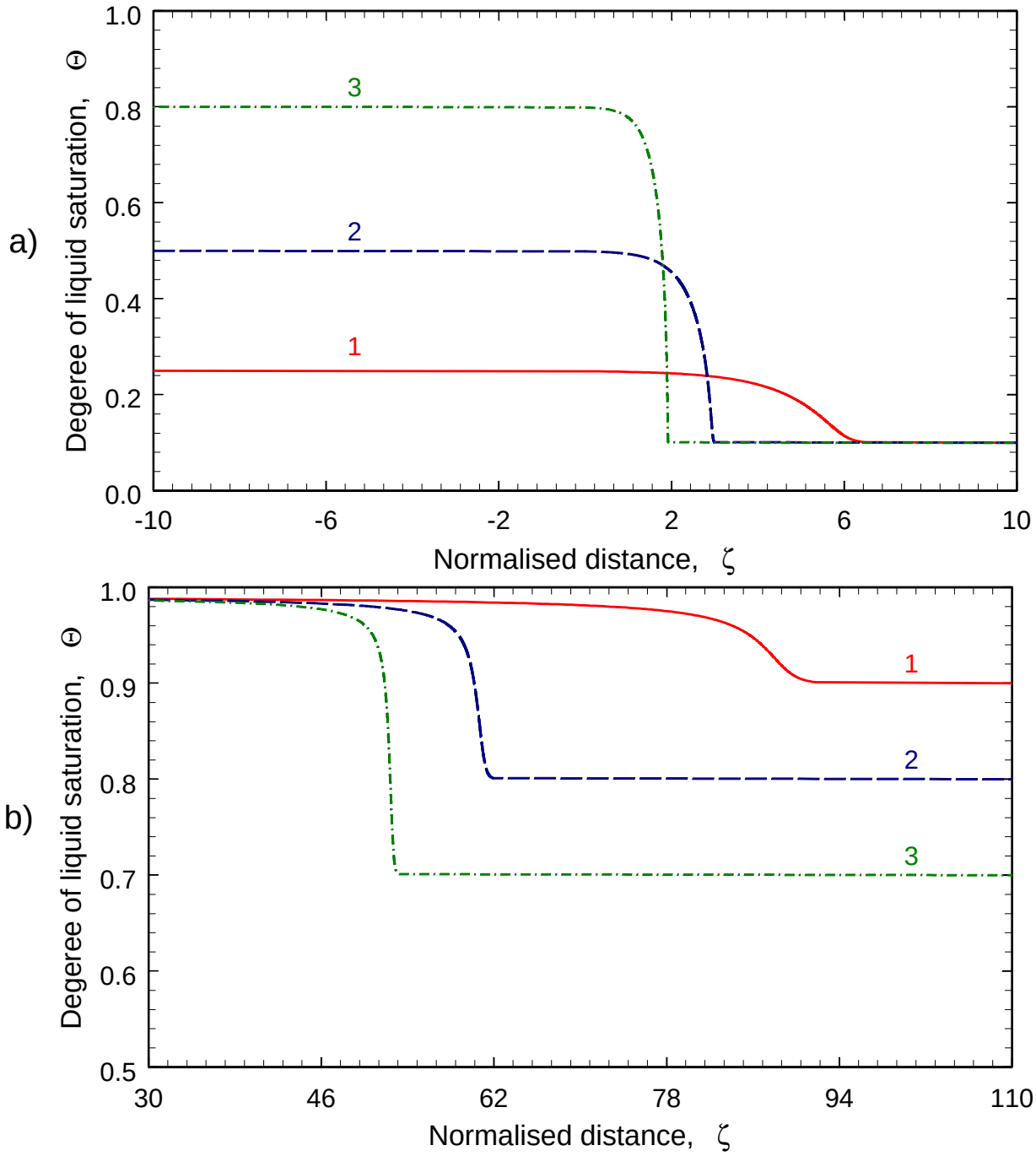

Figure 9: a) Travelling front profiles for the BC model for $\Theta_1 = 0.1$ and $\Theta_2 = 0.25, 0.5$ and 0.8. b) The same for the SF model for $\Theta_2 = 1$ and $\Theta_1 = 0.9, 0.8$ and 0.7.

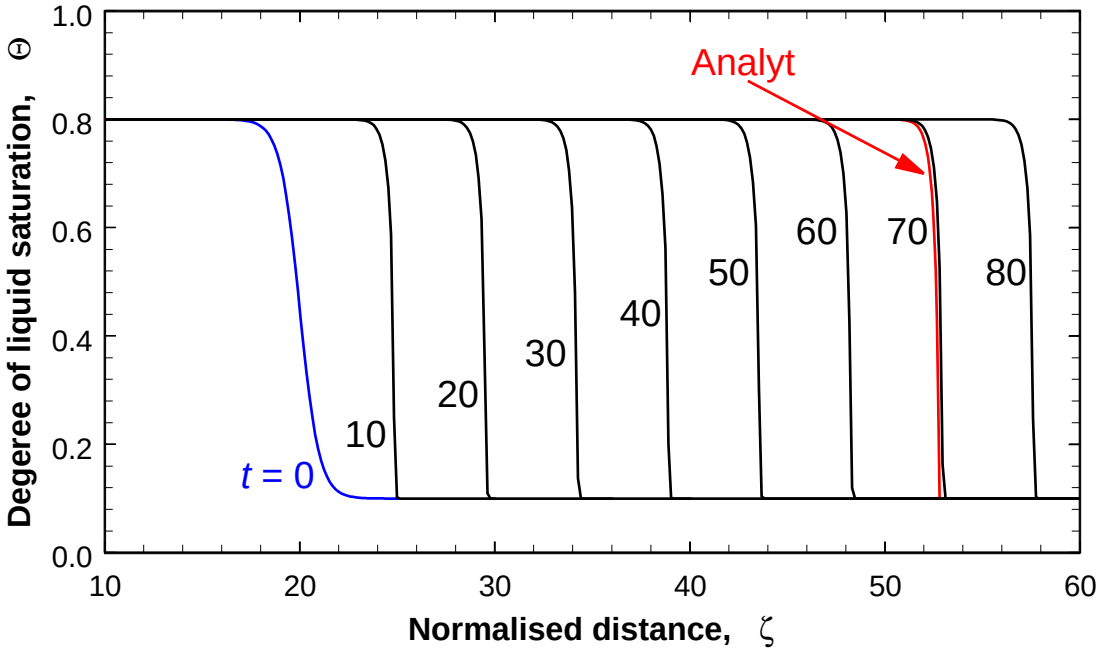

Figure 10: Travelling front solution for the BC model: evolution of an initial perturbation $\Theta(x,t)$ given by Eq. (42) for successive times $t = 0, 10, 20, \ldots, 80$. The analytical solution Eq. (40) is the line labelled "Analyt".

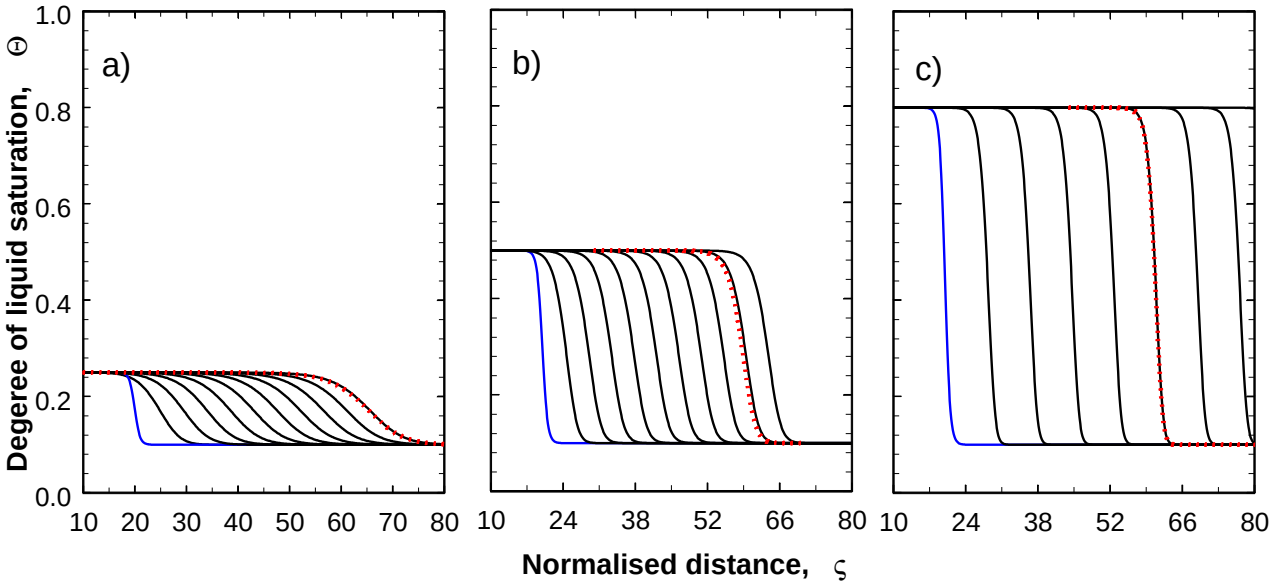

Figure 11: Travelling front solutions for the MvG model for $\Theta_1 = 0.1$ and a) $\Theta_2 = 0.25$; b) $\Theta_2 = 0.5$; c) $\Theta_2 = 0.8$. The plots show the evolution of an initial perturbation $\Theta(x,t)$ given by Eq. (42) for successive times $t = 0, 24, 48, \ldots$ for panel a) and $t = 0, 10, 20, \ldots$ for panels b) and c). The first curve starting from the left in each frame is the initial condition. The dotted lines show the corresponding travelling front solutions.

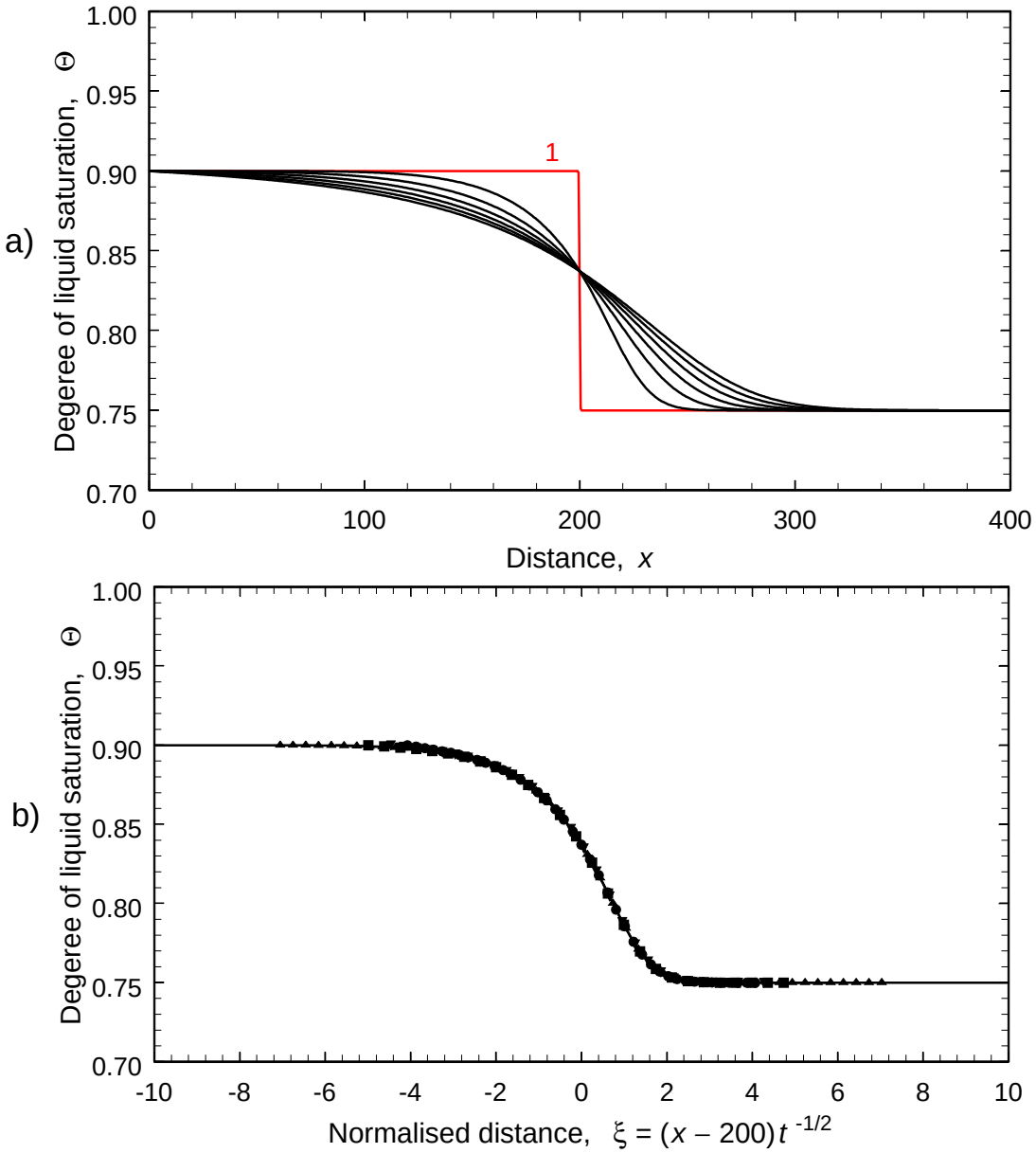

Figure 12: a) Evolution of the initial perturbation given by Eq. (42) for successive times: $t = 0$ (line 1), 400, 800, ..., 2400 for the imbibition case and the SF model with $\Theta_l = 0.9$ and $\Theta_r = 0.75$ ($a = 0.025$, $b = 1.001$). b) Plots of the solution $\Theta(x,t)$ shown in Fig. 12a as a function of the self-similar variable $\xi = \frac{x-200}{\sqrt{t}}$. The solid line shows the solution for $t = 400$ and the dotted lines with different symbols show solutions for other times. The self-similar analytic solution is also plotted and coincides with the numerical solution.